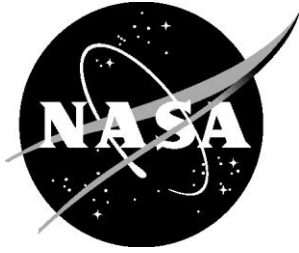


NASA/TM-20210011743



Relocatable 10 kW Solar Array for Lunar South Pole Missions

*Richard Pappa, Chuck Taylor, Jay Warren, Matt Chamberlain, Sarah Cook, Scott Belbin, Roger Lepsch, Dan Tiffin, and Bill Doggett
Langley Research Center, Hampton, Virginia*

*Martin Mikulas and Iok Wong
National Institute of Aerospace, Hampton, Virginia*

*Dave Long, Devon Steinkoenig, and Alejandro Pensado
Analytical Mechanics Associates, Hampton, Virginia*

*Joseph Blandino and Jerry Haste
Virginia Military Institute, Lexington, Virginia*

March 2021

NASA STI Program Report Series

Since its founding, NASA has been dedicated to the advancement of aeronautics and space science. The NASA scientific and technical information (STI) program plays a key part in helping NASA maintain this important role.

The NASA STI program operates under the auspices of the Agency Chief Information Officer. It collects, organizes, provides for archiving, and disseminates NASA's STI. The NASA STI program provides access to the NTRS Registered and its public interface, the NASA Technical Reports Server, thus providing one of the largest collections of aeronautical and space science STI in the world. Results are published in both non-NASA channels and by NASA in the NASA STI Report Series, which includes the following report types:

- **TECHNICAL PUBLICATION.** Reports of completed research or a major significant phase of research that present the results of NASA Programs and include extensive data or theoretical analysis. Includes compilations of significant scientific and technical data and information deemed to be of continuing reference value. NASA counterpart of peer-reviewed formal professional papers but has less stringent limitations on manuscript length and extent of graphic presentations.
- **TECHNICAL MEMORANDUM.** Scientific and technical findings that are preliminary or of specialized interest, e.g., quick release reports, working papers, and bibliographies that contain minimal annotation. Does not contain extensive analysis.
- **CONTRACTOR REPORT.** Scientific and technical findings by NASA-sponsored contractors and grantees.

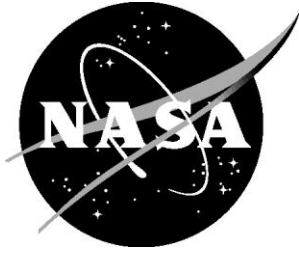
- **CONFERENCE PUBLICATION.** Collected papers from scientific and technical conferences, symposia, seminars, or other meetings sponsored or co-sponsored by NASA.
- **SPECIAL PUBLICATION.** Scientific, technical, or historical information from NASA programs, projects, and missions, often concerned with subjects having substantial public interest.
- **TECHNICAL TRANSLATION.** English-language translations of foreign scientific and technical material pertinent to NASA's mission.

Specialized services also include organizing and publishing research results, distributing specialized research announcements and feeds, providing information desk and personal search support, and enabling data exchange services.

For more information about the NASA STI program, see the following:

- Access the NASA STI program home page at <http://www.sti.nasa.gov>
- Help desk contact information: <https://www.sti.nasa.gov/sti-contact-form/> and select the "General" help request type.

NASA/TM-20210011743



Relocatable 10 kW Solar Array for Lunar South Pole Missions

*Richard Pappa, Chuck Taylor, Jay Warren, Matt Chamberlain, Sarah Cook, Scott Belbin, Roger Lepsch, Dan Tiffin, and Bill Doggett
Langley Research Center, Hampton, Virginia*

*Martin Mikulas and Iok Wong
National Institute of Aerospace, Hampton, Virginia*

*Dave Long, Devon Steinkoenig, and Alejandro Pensado
Analytical Mechanics Associates, Hampton, Virginia*

*Joseph Blandino and Jerry Haste
Virginia Military Institute, Lexington, Virginia*

National Aeronautics and
Space Administration

Langley Research Center
Hampton, Virginia 23681-2199

March 2021

The use of trademarks or names of manufacturers in this report is for accurate reporting and does not constitute an official endorsement, either expressed or implied, of such products or manufacturers by the National Aeronautics and Space Administration.

Available from:

NASA STI Program / Mail Stop 148
NASA Langley Research Center
Hampton, VA 23681-2199
Fax: 757-864-6500

Relocatable 10 kW Solar Array for Lunar South Pole Missions

Richard Pappa, Chuck Taylor, Jay Warren, Matt Chamberlain, Sarah Cook,
Scott Belbin, Roger Lepsch, Dan Tiffin, Bill Doggett
NASA Langley Research Center, Hampton, VA

Martin Mikulas, Iok Wong
National Institute of Aerospace, Hampton, VA

Dave Long, Devon Steinkoening, Alejandro Pensado
Analytical Mechanics Associates, Hampton, VA

and

Joseph Blandino, Jerry Haste
Virginia Military Institute, Lexington, VA

Deployable, relocatable, free-standing solar arrays are being developed to provide modular power for future lunar South Pole missions. Major design requirements for these arrays will be low mass, compact launch stowage, and highly reliable deployment and retraction. This paper presents a novel conceptual design for a 10 kW solar array to address these requirements referred to as the Relocatable Solar Array (RSA). Simply stated, the concept is a pair of solar cell blankets freely hanging from a horizontal cross arm supported by a vertical, slender, telescoping mast resting on a deployable tripod base. A major factor in simplifying the design is that the force exerted by lunar gravity is used to deploy and maintain extension of the hanging array blankets. A second major factor in achieving the desired low mass and high volumetric efficiency is that the array operates in the vacuum, low-gravity, lunar environment with no deployed vibration frequency requirement. Such a low-load environment enables use of extraordinarily slender and low mass structural members to support the hanging array blankets. This concept was developed, in part, to serve as a NASA reference solar array concept against which other proposed arrays can be compared.

I. Introduction

Solar arrays have been successfully used to generate electricity in a wide variety of space programs for over 50 years. Most of these applications involve arrays deployed in the zero-g environment of space, with the exception of a few small arrays on the surface of the Moon and Mars. The current application being studied is for fairly large arrays to be used near the lunar South Pole, where the Sun is always located within a few degrees of the horizon (Reference 1). For this application, the arrays must be vertical and free standing and be deployed in the lunar 1/6 g gravity field. Additional major requirements are that the array solar cell blanket must be elevated to 10 m above the lunar surface, must rotate to track the Sun through the 708 hr lunar day, and be capable of being retracted and relocated to an alternate site as needed.

Because the array must be capable of being retracted, an overarching desire for the conceptual design is to keep the system as mechanically simple as possible. Additional major requirements for a lunar exploration application are that the array be highly mass and volumetrically efficient. To deal with this new challenging set of requirements, a novel array referred to as the "Relocatable Solar Array" (RSA) is introduced in this paper as a NASA reference concept against which other concepts can be compared and understood.

Simply stated, the RSA is a pair of solar cell blankets free hanging from a horizontal cross arm supported by a vertical slender mast, all of which rests on a tripod base as shown in Figure 1. A major factor in simplifying the array is that the force exerted by lunar gravity is used to deploy and maintain extension of the hanging array blankets. A second major factor in achieving the desired low mass and high volumetric efficiency is that the resulting solar array operates in the vacuum, low-gravity, lunar environment with no structural frequency requirement. This environment allows the use of extraordinarily slender and low-mass structural members to support the hanging array blankets. The design parameters chosen for the current reference array are intentionally optimistic to provide understanding of the lower limit to achievable packaging volume and array mass. It should be noted that imposing a requirement that this array be fully operational on Earth without offloading part of its weight would result in a large penalty on both packaging volume and structural mass, and no such requirement is imposed.

The simultaneous desire to have a low mass and low package volume results in a somewhat paradoxical situation for the array design. The best way to reduce the mass of the tall support mast would be to decrease its thickness and increase its diameter to provide a greater moment of inertia. Such an approach is commonly done using open-grid walls. However, increasing the mast diameter increases the required stowage volume. Thus, a tradeoff must be made between low mass and low stowage volume. For the current reference design, emphasis is placed on achieving the lowest possible practical stowage volume. This approach places a high emphasis on innovative mechanism design features, whereas lower mass may be achieved using extremely high-performance materials. For the current reference design, a volumetric packaging goal of 20 kW/m^3 , including an integrated tripod support, was selected. A performance-enhancing feature omitted in this design is the use of tension stiffening cables. Although their use could improve mass and packaging metrics, they were not considered in this study.

The main objective of this paper is to show that a plausible design exists for a 10 kW South Pole lunar array having a 20 kW/m^3 volumetric packaging efficiency. The results of the study were also aimed at providing dimensional and force requirements for to-be-developed hardware such as joints, latches, actuators, and slender structures. Predicted solar array temperatures and resulting deformations of the structure at the lunar South Pole are also discussed.

The solar array properties and assumptions used for sizing structural members in the study are first described to assist in understanding the somewhat unique design approach. In this design approach, an aggressive solar array power per unit volume (PPV) goal is used as a constraint, which directly affects the concept configuration as well as member sizing. Next, an overview is presented of the array deployment sequence, followed by an overview of the resulting array physical characteristics. To meet the challenging PPV goal, it was necessary to develop a novel deployable support tripod. Finally, because of the preliminary nature of the current design, a short discussion is presented of available volumetric design margins as well as promising areas for further design improvements.

II. Solar Array Properties and Assumptions

A schematic of the 10 kW solar array concept considered in this paper for lunar South Pole missions is shown in Figure 1. Because of potential sunlight blockage caused by unknown details of the lunar landing site terrain and periodic changes in the elevation of the Sun, a requirement that the array must be elevated 10 m above the surface has been imposed and represents a major design driver. The preliminary dimensions for the array were determined from the launch volumetric stowage goal and the assumed array properties as shown in Table 1. In addition, the Moon rotates on its axis once every Earth month, which is about 0.5° per hour. A thermal analysis presented in Appendix B indicates the resulting temperature gradient across the vertical support mast will be approximately 210°C . This large temperature gradient provides another constraint in the design process. To minimize monthly differential movement between the vertical mast and the solar array blankets, the azimuth rotation mechanism required to track the Sun is placed at the bottom of the mast as indicated in red in Figure 1. This placement of the rotation mechanism ensures the array and vertical mast rotates as a unit with the same surface always facing the Sun. Since this large, vertically standing array is specifically meant for use in the vicinity of manned lunar surface operations, it is imperative the device be safely robust in terms of structural strength and vertical stability. To deal with this safety condition, a

requirement is established in the current paper that the array must be capable of deploying on unprepared ground with a slope of up to 15° and sufficient automatic leveling capability to avoid structural failure or tipping over.

Although the 20 kW/m^3 volumetric packaging goal is much lower than the 60 kW/m^3 goal of Reference 2, it represents a major design challenge for the following three reasons. First, a deployable tripod stand must be included in the package for free-standing surface operations. Second, the solar cell blankets are slightly thicker than the absolute minimum to account for a slight stiffening of the Z-folded panels of the blanket. Third, since the area of solar arrays increases as the square of dimensions, the structural support mast of the smaller array considered herein represents a larger percentage of volume than the large arrays considered in Reference 2. Thus, scaling laws dictate that the support structure is a larger percentage of the array package. The packaging efficiency goal of 20 kW/m^3 selected in this paper imposes a requirement that the complete 10 kW solar array must be contained within a stowed volume no greater than 0.5 m^3 . A third major design driver is the array must be capable of relocation. This relocation requirement dictates that the array must be retracted, moved, and then redeployed multiple times. To confidently meet this challenging relocation requirement in a reliable fashion, it is necessary to keep the array system as mechanically simple as possible.

III. Array Deployment Sequence

RSA Surface Positioning

The deployment and retraction concept considered in this paper is shown in the six deployment steps of Figures 2 and 3. In the first step shown in Figure 2, the packaged RSA is unloaded from the lunar lander and moved to the desired operation site. It is assumed the RSA is unloaded from the lander by some sort of crane device and it is transported to its operational site by a rover. The RSA could also potentially be deployed directly on the lander.

Tripod Deployment

In the second step, the tripod legs are deployed into position as shown in Figure 2. The deployment of the tripod legs is accomplished using linear actuators that are indicated as the red members in the figure. It is assumed these actuators enable the tripod to conform to as much as a 15° slope of the terrain as well as keep the deployed mast plumb if regolith settling occurs. Although the initial assumption is that these actuators will be some arrangement of electrical screw jack devices, their detailed orientation and design is beyond the scope of this conceptual paper. In the current manifestation of the support tripod, the nested linear actuators are placed under the legs so they are loaded in tension. In this configuration, it is possible the actuators could be winch-driven cables. The potential advantage of using cable actuators would be to provide a further reduction in packaging volume.

Vertical Mast Deployment

The third step of the deployment process is to telescope the mast vertically to its upright position as shown in Figure 2. As was the case for the tripod base, the details of the telescoping actuation are beyond the scope of this paper. In Reference 2, telescoping masts deployed by either screw jacks or deployable booms are discussed. An alternate attractive approach for lunar surface applications is to use a rover-mounted, simple elongating tool that would engage, extend, and lock each telescoping section sequentially to accomplish the mast deployment. The advantages of using such a device are three-fold. First, the actuator would not impose a major diameter constraint on the telescoping sections. Second, the deployment tool could be used for multiple arrays. Third, the tool size could be adjusted to deploy larger masts if needed for solar arrays above 10 kW .

Stowed Array Deployment

As shown in the fourth deployment step of Figure 3, the stowed array canisters are rotated to a horizontal position using either a simple cable system as shown or a gear-driven actuator. Because of the low lunar gravity, this is not a major operation.

Blanket Deployment and Retraction

The deployment of the Z-folded array blankets is accomplished and controlled with extendable cords using the force exerted by lunar gravity as indicated in Step 5 in Figure 3. Since the blanket operates in the extremely benign lunar environment, no structural frequency constraint is imposed, and the blanket is simply freely hanging from the upper cross arm. This greatly simplifies the array design as compared to zero-g space applications, which typically require blanket-stiffening springs to achieve a minimum deployed vibration frequency.

Completely Deployed Array

The completely deployed array is shown as Step 6 in Figure 3. It is anticipated the Z-folded array panels will not be fully extended resulting in a slight angle in the panels. The purpose of not extending the solar cell blanket fully is to assist the retraction process by ensuring the panels retract correctly. Alternatively, hinge-line torsional springs can be used to enforce proper folding.

IV. RSA Preliminary Design Overview

Array Blanket Mass

In Figure 4, an overview is shown of a 10 kW RSA design after preliminary sizing. It should be noted that the initial sizing effort resulted in a support structure with extraordinarily slender members. In the upper left portion of the figure, the 50 kg mass loading that must be supported by the 16 m high mast is shown. This 50 kg mass is composed of 36 kg for the 36 m² solar array blanket with a 14 kg allowance for the blanket upper and lower cross arm support members and the required winch-and-cable blanket deployment system. The right-hand sketch shows this 50 kg in the 1/6 g lunar gravity produces a downward force of only 80 N (18 lb), which must be supported by the mast.

Mast Deformation and Strength Analysis

In Appendix A, deformation and strength analyses are conducted of the RSA. To understand limiting deformations and stresses to which the array will be subjected, the array is simplified as a constant diameter, 16 m long mast with gravitational loads as described in the previous section. To quantify potential deformations and stresses, a conservative assumption is made that the array must safely withstand a tilt angle of 15°. In addition to gravity loading, the solar thermal loads and resulting deformations presented in Appendix B are also discussed.

Tripod Leg Design Considerations

In Appendix C, a strength analysis is conducted of the RSA tripod support legs subjected to the gravity loads as shown in Figure 4. The geometry and length of the tripod legs are dictated by a requirement that the array not tip over on a 15° slope. Although this requirement may be quite conservative, it was chosen because crew might come near the free-standing solar array at some point. Details of the 15° tipping analysis are presented in Appendix D.

Launch Package Size and Volumetric Efficiency

As a result of the preliminary sizing design, the resulting 10 kW RSA stows in a 0.5 m³ volume as shown in the lower left of Figure 4. Further details of the stowed array are presented in a subsequent section. For reference purposes, this packaged RSA is shown in two different orientations inside a 5 m diameter launch shroud as shown in Figure 5. Since the RSA only occupies less than 1% of the shroud volume, numerous arrays could be carried on a single launch.

The major member-sizing changes from the preliminary RSA cartoon sketch shown in Figure 1 result from considering the low loading of the lunar gravity for member sizing as well as imposing the volumetric packaging goal of 20 kW/m³. The resulting slender support structure is shown in the three sketches of Figure 6. The cross-arm support members for the blankets have been assumed to be 2.5 cm (1 in) thick for a slenderness ratio of approximately 120. The cross arms also represent the canister required to contain and protect the Z-folded blanket panels during launch. The mast diameter of 0.15 m (6 in) results in a slenderness ratio of approximately 107 for the 16 m height. The selected tripod leg length of 4 m with a diameter of 3 cm (1.2 in) results in an aspect ratio of 130. These slenderness ratios are

at least twice those normally accepted as good practice for terrestrial civil engineering structures. The major justification for the acceptance of such high slenderness ratios is low lunar gravitational forces as compared with Earth gravitational forces. Although these extraordinarily high slenderness ratios enable the volumetric efficiency goal of 20 kW/m^3 , testing will be required to ensure their adequacy.

15° Terrain Tilt Requirement

The severity of the tilt requirement is indicated in Figure 7. This 15° slope requirement is dealt with in two different ways. First, in a previous section an analysis was conducted to ensure the strength and stiffness of the mast was adequate to withstand a 15° tilt. Second, the design of the tripod deployment actuators must be such that they have adequate extensibility to be capable of handling a 15° slope as shown in Figure 7.

V. Tripod Deployment Design Concept

A top view schematic of the mast and tripod legs is shown in Figure 8. Each leg consists of two tubes with a centrally nested linear actuator. The reason for this novel arrangement is to minimize the total packaged diameter to meet the 20 kW/m^3 stowage goal. Note that the hinge lines of the tubes and actuators are intentionally offset to eliminate mechanism lockup during deployment. A side view of the two-tube leg and linear actuator is shown in Figure 9 for two angular deployment orientations. These partial schematics are only conceptual in nature, as the specific design and dimensions are left for future work.

As mentioned previously, this particular arrangement lends itself to the application of winch-driven cable actuators since they are in tension for the operational configuration. The use of cable actuators would require return force springs to hold the legs in their stowed geometry.

VI. Packaged RSA Configuration

A top view of the final compactly stowed RSA is shown in Figure 10. The two 3 m long, solar array canisters are packaged on each side of the stowed 0.15 m (6 in) diameter mast and associated tripod legs. A side view of the package is shown as Step 1 in Figure 2. As can be seen in the schematic, the Z-folded solar cell blankets shown as blue, occupy a small fraction of the volume. After sizing for the central mast and nested legs, the 20 kW/m^3 volumetric packaging goal was finally met by constraining the array blanket support cross arms to a thickness dimension of 2.5 cm (1 in). Although this cross-arm design results in a slender support structure, the $1/6 \text{ g}$ induced loads in the blankets are quite low.

VII. Volumetric Design Margins

As currently configured and sized, there appears to be little margin for incorporating launch support hardware, deployment and latching mechanisms, power harnesses, and other unanticipated volumetric needs while meeting the 20 kW/m^2 goal. The most likely paths for achieving further volume reduction would be to reduce the thickness of the array support cross arms or reduce the mast diameter. An attractive area to pursue is that of using an external robotic tool to extend the mast segments sequentially. This approach has the potential advantage of eliminating a dedicated internal deployer, thus reducing the array mass as well as reducing the required mast diameter. These items are areas for further investigation.

VIII. Conclusions

Deployable and relocatable, free-standing, vertical solar arrays are being developed for future lunar South Pole missions. Major design requirements for these arrays will be low mass, compact launch stowage, and highly reliable deployment and retraction performance. In the present paper, a novel conceptual design referred to as the Relocatable Solar Array (RSA) is presented for a 10 kW solar array to satisfy these requirements.

To achieve the desired mass and volumetric metrics, the following three novel features were incorporated into the design:

- First, the solar cell blankets are freely hanging from cross arms with no additional stiffening. This feature greatly simplifies the required structure and mechanisms.
- Second, all structural members are sized to operate in the 1/6 g low force lunar environment. This condition results in structural members with length-to-depth slenderness ratios over twice those commonly acceptable for terrestrial civil engineering structures.
- Third, the tripod support base is formed from three deployable truss legs that package compactly around the central support mast. The required compactness of the tripod is achieved using legs with nested linear actuators.

Analytical results are presented for an example 10 kW array that show large margins for gravity-induced stresses and buckling loads, and that gravity and thermal induced tip deflections of the vertical support mast are a fraction of the tube diameter. Although this preliminary array design shows promise for efficient volumetric packaging, considerable detailed design, development, and verification will be required for the associated deployment mechanisms to ensure the array meets other design requirements for all operating environments including launch loads and thermal extremes.

IX. Acknowledgments

This work was funded by the Vertical Solar Array Technology (VSAT) project sponsored by NASA's Game Changing Development Program in the Space Technology Mission Directorate. The initial concept for the Relocatable Solar Array (RSA) was developed by co-author Martin Mikulas of the National Institute of Aerospace.

X. References

¹Pappa, Richard S., et al., "Solar Power for Lunar Pole Missions," Space Power Workshop, April 2019, <https://ntrs.nasa.gov/search.jsp?R=20200000285>.

²Mikulas, Martin M., et al., "Telescoping Solar Array Concept for Achieving High Packaging Efficiency," AIAA SciTech Forum, January 2015, <https://ntrs.nasa.gov/archive/nasa/casi.ntrs.nasa.gov/20150006022.pdf>

³Johnson, Robert R., et al., "Thermal Expansion Properties of Composite Materials," NASA Contractor Report 165632, July 1981, <https://ntrs.nasa.gov/citations/19810023033>.

⁴Thornton, Earl A., "Thermal Structures for Aerospace Applications," AIAA Education Series, J.S. Przemieniecki Series Editor in Chief, AIAA, Inc., Reston, VA, 1996, pp 356-357.

⁵Thornton, Earl A., "Thermal Structures for Aerospace Applications," AIAA Education Series, J.S. Przemieniecki Series Editor in Chief, AIAA, Inc., Reston, VA, 1996, pp 118-121.

⁶https://www.nasa.gov/mission_pages/station/structure/elements/solar_arrays.html, NASA ISS solar arrays.

Symbols and mast values used in Appendices A and B.

L	Length of mast, 16 m (640 in)
c	Specific heat of mast material
D	Maximum D of mast tube, 15 cm (6 in)
h	Thickness of mast tube, 2 mm (0.08 in)
k	Thermal conductivity of mast tube material
ρ	Density of mast tube material
E	Modulus of elasticity of mast material, 130 GPa (19 msi).
I	Tube moment of inertia
$v(L)$	Tip deflection with a 15° mast tilt
σ	Stefan–Boltzmann Constant
σ_{root}	Maximum root stress with 15° mast tilt
$F_{mast,Space}$	Radiation View Factor between mast tube and space
$F_{mast,Regolith}$	Radiation View Factor between mast tube and surrounding Regolith
P_{Euler}	Euler buckling load of uniform diameter and thickness, cantilevered mast
P_V	Vertical compressive load acting on mast
P_L	Lateral component of load acting on. mast
M_{root}	Moment a root of mast due to P_L
M_{tube}	Mass of tube
M_T	Thermal moment of the mast tube
q_{solar}	Solar Constant
α	Thermal absorptivity of mast surface
α_T	Coefficient of thermal expansion
ϵ	Emissivity of mast surface
π	Pi
τ	Thermal time constant of the mast
T_m	temperature deviation from average mast temperature.
\bar{T}_{mast}	Average mast temperature.
ΔT	Temperature gradient across the mast tube diameter.
T_{Space}	Temperature of background Space
$T_{Regolith}$	Temperature of surrounding Regolith

Appendix A. Bending Stresses and Deformations of the RSA 16-Meter Mast

Mast Sizing Considerations

The mast is assumed to be a composite tube with an elastic modulus of 130 GPa (19 msi) and an average wall thickness, h , of 2 mm (0.08 in). The reason for this rather thick wall is to provide robustness against damage in an active, potentially crewed, operational area. In this study, the modulus of the mast was limited to 130 GPa (19 msi) due to the composite layup required to achieve a low coefficient of thermal expansion. The assumed density of the mast tube, ρ , is 1600 kg/m³. Although a 0.1 m (4 in) diameter mast would be capable of satisfying all anticipated design conditions, telescoping requirements will likely dictate that the mast diameter, D , must be at least 0.15 m (6 in). This is due to the need to nest the multiple telescoping sections as well as a diameter allowance for some type of internal extension actuator.

To determine the strength and stiffness adequacy of the assumed mast tube dimensions, a structural analysis was conducted of the Euler buckling, as well as the root stress and mast tip deflection of the 16-meter-long mast subjected to the 80 N compressive load, P_V , as shown in Figure 4. The root stress and resulting tip deflection were calculated assuming a mast tilt of 15°.

The Euler buckling of the 16 m long mast subjected to an axial compressive tip load is

$$P_{Euler} = \frac{\pi^2 EI}{4L^2} \quad (A1)$$

Substituting the assumed mast values into Equation A1 yields a buckling load of 3564 N, which is well above the applied compressive load of 80 N.

The lateral component, P_L , of the 80 N compressive load, P_V , acting on the tip of the mast at a tilt of 15° is

$$P_L = P_V \sin(15^\circ) = 20.7 \text{ N} \quad (A2)$$

This lateral load, P_L , causes a bending moment M_{root} and a bending stress, σ_{root} , at the root of the mast as well as a tip deflection, $v(L)$. The equation for the root bending stress is

$$\sigma_{root} = \frac{M_{root} D/2}{I} = \frac{P_L L D/2}{I} = 8.8 \times 10^6 \frac{\text{N}}{\text{m}^2} = 1284 \text{ psi} \quad (A3)$$

where, $I = \frac{\pi D^3 h}{8}$, is the moment of inertia of the mast tube. This value of the root stress is well below the allowable stress for composite that would be over 50,000 psi.

The lateral deflection of the mast tip is given by

$$v(L) = \frac{P_L L^3}{3EI} = 7.6 \text{ cm (3 in)} \quad (A4)$$

This lateral tip deflection is only about half of a diameter of the mast and would not impose a problem with the operation of the vertical solar array. The mass of the assumed constant diameter mast tube is given by

$$M_{tube} = \pi D h L \rho = 24.9 \text{ kg} \quad (A5)$$

In summary, limiting deformation and load analyses were conducted to evaluate the robustness of the assumed telescoping structural concept. An analysis of the mast root stress and tip deflection resulting from a 15° tilt of the RSA is presented as a conservative design case. As can be seen from the results, the root bending stress is only 9 MPa (1300 psi), which is well below the allowable for composites, and the maximum tip deflection is only 7.6 cm (3 in). Assuming that the tube has a constant diameter of 0.15 m (6 in) and a thickness of 2 mm (0.08 in) yields an Euler buckling load for the 16 m long mast of ~3600 N (870 lb). This load is considerably higher than the tip-mass-induced load of 80 N (18 lb). For this reason, negligible beam/column interaction will occur between the tip load and small tip displacements that may result from imperfections, small tilts, or thermal distortions.

Thermal Loading and Distortions

A further check of the design is the maximum tip deflection due to thermal gradient from solar heating and deep space cooling. This analysis is presented in Appendix B. In the current study, it is assumed that a Coefficient of Thermal Expansion (CTE) of approximately $\pm 0.18 \times 10^{-6}/^\circ\text{C}$ ($0.1 \times 10^{-6}/^\circ\text{F}$) is readily obtainable for a graphite epoxy composite mast. Thus, the resulting thermal tip deflection of a 0.15 m diameter mast would be approximately 2.5 cm as shown in Figure B2. Reference 3 discusses the practicality of achieving extremely low values of CTE in composites and mentions it is not feasible to specify a CTE less than $\pm 0.09 \times 10^{-6}/^\circ\text{C}$ ($0.05 \times 10^{-6}/^\circ\text{F}$) for practical laminate designs. Thus, further reduction in temperature-induced tip deflection, if needed, would probably require specialized thermal control treatments.

Appendix B. Thermal Distortion Considerations

Thermal bending of the RSA vertical support mast will occur due to a temperature gradient across the diameter. At the lunar South Pole, the Sun, which is near the horizon, will heat one side of the mast while the other side will be quite cool due to exposure to deep space and the lunar surface. The heating geometry is shown in Figure B1. The component of the solar radiation incident on the mast surface is a function of position, θ , around the circumference of the mast. The temperature gradient across the diameter of the mast produces a thermal moment as discussed in Reference 4. The thermal moment will cause bending of the mast resulting in a tip displacement that must be accounted for in the design. For a thin-walled tube, the thermal moment is found from

$$M_T(t) = \pi E \alpha_T \frac{\Delta T(t)}{8} D^2 h \quad (\text{B1})$$

where $\Delta T(t)$ is the temperature gradient across the mast diameter, α_T is the coefficient of thermal expansion, D is the mast tube diameter, h is the wall thickness, and E is the elastic modulus. For a mast at the lunar South Pole, evaluating Equation (B1) at steady state will give the maximum thermal moment.

The quasi-static tip displacement, $v(L)$, of a vertical cantilever beam with applied tip moment, M_T , is found from

$$v(L) = \frac{M_T L^2}{2EI} \quad (\text{B2})$$

Details of the derivation of Equation (B2) can be found in Reference 4. For a thin-walled tube, the moment of inertia is

$$I = \frac{\pi D^3 h}{8} \quad (\text{B3})$$

Combining Equations (B1), (B2), and (B3) gives a simplified equation for determining the mast tip displacement due to thermal bending of a vertical, cantilever mast. The equation is based on the mast length, coefficient of thermal expansion, mast diameter, and temperature gradient across the diameter. The simplified equation is

$$v(L) = \frac{\alpha_T \Delta T L^2}{2D} \quad (\text{B4})$$

Equation (B4) can be used to find the maximum displacement at steady state, as this state coincides with the maximum temperature gradient and maximum thermal moment.

Figure B2 shows the relationship between tip displacement vs. coefficient of thermal expansion of a mast 16 m in height with 0.1 m, 0.15 m, or 0.2 m diameter and a 2 mm wall thickness. The figure shows the importance of minimizing the CTE in order to minimize tip deflection. For reference, the CTE of an M55J/934 lamina is shown in the figure.

The thermal moment, described in Equation (B1), is a function of the coefficient of thermal expansion and the thermal gradient across the boom diameter. Materials with a low coefficient of thermal expansion often have a low thermal conductivity. These are typically composite materials. Although a composite material can be fabricated to have a low coefficient of thermal expansion, the temperature gradient may be large due to a low thermal conductivity. Both values are important for predicting bending.

To find the temperature difference across the mast tube an approach similar to that presented in Reference 5 is used. Two coupled differential equations describe the temperature of the mast. Equation (B5) describes the average temperature of the mast. The average temperature does not influence the thermal moment. The second equation,

Equation (B6), describes a temperature variation away from average mast temperature, \bar{T}_{mast} . The perturbation temperature, $T_m(t)$, is a time-varying temperature that is superposed on the average mast temperature. The perturbation temperature is caused by asymmetric heating of the mast. The perturbation temperature causes the temperature gradient across the diameter of the mast tube that creates a thermal moment.

$$\frac{d\bar{T}_{mast}}{dt} + \frac{\sigma\epsilon}{\rho ch} \bar{T}_{mast}^4 = \frac{1}{\rho ch} \left[\alpha \frac{q_{solar}}{\pi} + F_{mast,space} \sigma \epsilon T_{space}^4 + F_{mast,regolith} \sigma \epsilon T_{regolith}^4 \right] \quad (B5)$$

$$\frac{dT_m}{dt} + \left(\frac{4k}{\rho c D^2} + \frac{4\sigma\epsilon}{\rho ch} \bar{T}_{mast}^3 \right) T_m = \frac{\alpha q_{solar}}{2\rho ch} \quad (B6)$$

In the above equations, σ is the Boltzman constant, ϵ is the emissivity, α is the absorptivity, ρ is the density, c is the specific heat, q_{solar} is the solar constant, and the radiation view factors are $F_{mast,space}$ and $F_{mast,regolith}$. For determining bending, only the perturbation temperature, $T_m(t)$, is of concern as this causes the thermal moment and therefore bending of the mast.

The solution to Equation (B6) is

$$T_m(t) = \frac{\alpha q_{solar}}{2\rho ch} \tau \left(1 - e^{-\frac{t}{\tau}} \right) \quad (B7)$$

At steady state, Equation (B7) becomes

$$(T_m)_{ss} = \frac{\alpha q_{solar}}{2\rho ch} \tau \quad (B8)$$

where

$$\frac{1}{\tau} = \frac{4k}{\rho c R D^2} + \frac{4\sigma\epsilon}{\rho ch} \left(\frac{\alpha q_{solar}}{\pi\sigma\epsilon} \right)^{3/4} \quad (B9)$$

The thermal gradient across the diameter of the mast, which is used in Equation (B4) to find the tip displacement of the mast is

$$\Delta T = (2T_m)_{ss} \quad (B10)$$

An example of predicted thermal gradients is presented for graphite epoxy. Table B1 presents the thermal properties, and Table B2 gives the corresponding temperatures for the Sun facing and cold sides of the mast. The solar constant is taken as $q_{solar} = 1367 \frac{W}{m^2}$. Table B2 shows that for a material with a low thermal conductivity, the thermal gradients can exceed 220 K (400 °F).

Appendix C. Gravitational Loads in the RSA Support Tripod Legs and Actuators.

Tripod Leg Sizing Considerations

As can be seen in the lower right of Figure 4, the gravity-induced load on the tip of each leg is only 66 N (15 lb). A free-body diagram of the loads in each leg is presented in Appendix C, Figure C1. This analysis assumes the actuators extend to the end of the support leg whereas they will probably only extend to about $\frac{3}{4}$ of the leg length in the final design. The resulting loads in the tripod members are sufficiently low that the current approximate analysis is adequate to establish preliminary member sizing.

The gravity-induced loads in the tripod legs and actuators are shown parametrically in Figure C2. For reference, the Euler buckling load of a 3 cm (1.2 in) diameter, 4 m long leg fabricated of 240 GPa (35 M psi) composite material is over 4400 N (1000 lb). As shown in Figure C2, the induced load from the RSA mass in the lunar 1/6 g is less than 900 N (200 lb) depending upon the final tripod geometry. Although the legs are unusually slender, in the low-force lunar environment, there exists a comfortable margin above buckling. The nested linear actuators could be placed above the legs; however, this would be an additional design concern for the slender actuators since they would now be subjected to compression. In the current configuration, another option may be to use winch-actuated cables as actuators since they are always in tension.

Appendix D. Tripod Size as Dictated by Array Tipping Considerations

As discussed previously, a conservative requirement is imposed that the array not fail on a terrain slope of 15°. In this appendix, a study is conducted of the tripod size required such that the array would not tip over on a 15° slope. The top view of the legs of a tripod array are shown in Figure D1, while a simple tipping model of the array is shown in Figure D2. As indicated in Figure D2, the metastable tipping condition is met when the position of the array center-of-gravity (CG) reaches the outermost point of the base support. The angle for this metastable condition is shown in Figure D3.

A major observation from Figure D1 is that the outer-most point of the base is a strong function of the azimuth angle of the tripod relative to the local terrain slope. For this reason, the most stable array condition will be for the case in which one of the legs is pointed toward the steepest downward slope of the local terrain. As can be seen in Figure D1, the distance from the center of the tripod to the tipping point can vary by as much as a factor of two depending upon the azimuth rotation relative to the local terrain slope. For this reason, it would be desirable to provide array placement operational instructions that clearly describe this situation.

The current example RSA has a total mass of 120 kg with a mass breakdown shown in Figure 4. The approximate CG of this array is 9.5 m above the base. An exact location of the CG is not possible because of the approximate nature of the assumed value and location of the tripod mass. From the metastable angle equation presented in Figure D2, this dictates that the tripod legs must extend out approximately 3 m from the center. In the current design, it is assumed the tripod legs are almost 4 m long to provide the necessary 6 m diameter footprint for stability of the 16 m tall vertical array. Alternate solutions for obtaining adequate stability for the array could be to provide additional mass (batteries perhaps) at the base to lower the CG or to anchor the base to the terrain. Considerations of those options are beyond the scope of the paper.

Appendix E. Reduced Length of Packaged Array

A potential concern for the RSA model discussed in this paper is that the stowed array length may be too long for some applications. Although the current array stows in a volume of only 0.5 m³, the aspect ratio of the packaged array is such that the stowed array package is almost 4 m long as shown in Figure 5. The packaged length of the array is dictated by the 3 m length of the canisters that house the two drop-down blankets as well as by the 4 m long tripod support legs selected for vertical stability as discussed in Appendix D.

One possibility for reducing the stowage length from 4 m to 3 m is to shorten the tripod legs by telescoping. Although this could provide a 25% reduction in package length, some additional mechanical complexity is added. Another possibility for reducing the array packaged length would be to provide an additional fold in each side of the drop-down blankets to decrease their packaged length to 1.5 m. The deployment sequence of such an array concept is shown in Figure E1. Although this change to four blankets nicely reduces the packaged blanket canister length to 1.5 m, it results in two major impacts on the two-blanket design. First, twice as many telescoping segments will be required. The increase in number of telescoping sections will increase the mast diameter as well as add mechanical complexity to the system. Second, the achievement of a 6 m diameter tripod footprint from a 1.5 m long stowed package will result in a significant increase in tripod deployment complexity.

In the present paper, emphasis has been placed upon providing several notional designs with enough engineering analysis to provide an awareness of major design challenges. Detailed trade-offs of packaging volume, mass, and deployment complexity are beyond the scope of the current study.

Appendix F. Concept for Wiring Harness Extension Cord

The requirement to support the 10 KW lunar South Pole solar array at least 10 m (400 in) above the surface presents a new design challenge. This additional elevation requirement introduces the need for an extension harness cord to bring the 10 kW power from the array blanket down to the surface. Two major design goals for the RSA are to obtain compact packaging ($>20 \text{ kW/m}^3$) as well as a retractable capability. Although $>20 \text{ W/m}^3$ appears to be readily achievable for zero-g solar array applications as discussed in Reference 2, the addition of a large support base as well as the necessary additional power harness extension cord represent additional challenges to obtaining the compact packaging goal. In Appendix C, the support tripod leg members were sized to minimize packaging volume. In this appendix, a notional concept is introduced to minimize the impact of the 8 m long power extension harness on packaging volume and to provide the desired retractability performance.

The concept considered in this appendix for the wiring harness extension cord is similar to the primary harness used on the NASA ISS solar array as shown in Figures F1 and F2 from Reference 6. The extension power cord is basically a Z-folded flat and thin wiring harness that is capable of being stowed within the available volume of the bottom cross arm of the solar array blanket so that no penalty on the packaging volume is incurred. The solar array blanket lower cross arm is assumed to have a U-shaped channel cross-section with a depth of 5 cm (2 in) and a width of 30 cm (12 in). Since the tripod support base is about 2 m (80 in) high and the length of the vertical stowed array package is an additional 3 m (120 in) long, the length of the harness remaining to be deployed is only about 5 m (200 in) long. Thus, the required length of the deployable Z-fold harness cord will only be about 5 m (200 in).

To achieve the packaging within the 2-inch-thick lower cross arm, the following assumptions on the wiring harness are made based upon preliminary design. The width and thickness of the harness are such that the Z-folded harness will lay within the dimensions of the 2-inch-thick by 12-inch-wide U-shaped lower cross arm. In this appendix the wiring harness is assumed to be 15 cm (6 in) wide and less than 1 mm (0.04 in) thick. If each Z-fold is 0.5 m (20 in) long, 10 layers of the folded harness will be required to be stowed. The packaged thickness of such a harness will only be about 1 cm (0.4 in) and would easily stow within the thickness of the lower cross arm so that no additional required volume penalty would result.

The primary motivation for this type of harness is that it enables highly efficient, compact packaging of a solar array power harness without experiencing extreme folding of the wiring material. The wiring geometry must be chosen such that the deployment and packaging of the harness accomplished within the elastic behavior of the harness over the operational temperature range. For lunar South Polar applications, the unheated harness temperature in the shade could possibly be as low as 40 K ($-380 \text{ }^\circ\text{F}$).

Notional deployment sequence sketches for the 10 kW solar array including the Z-folded harness are shown in Figures F3 and F4. In Figure F3, the telescoping central mast is shown to have fully deployed the array blanket and is just beginning to pull out the orange Z-folded wiring harness. In Figure F4, the array blanket and Z-folded harness are shown as fully deployed. The Z-folded harness is left in a slightly zig-zag shape to ensure a correct initial geometry for kinematic retraction. A summary of the deployed array dimensions is shown in Figure F4.

Although not shown, it may be necessary to provide pretensioned cables through eye loops to properly guide the Z-folded panels during retraction. In this appendix, the wiring harness is only considered as far down as the red rotary joint. A tradeoff between the use of slip rings or rewinding the array every 180° to bring power across the rotary joint is not addressed in this paper.

Table 1. Solar Array Design Parameters

Power per unit volume of complete array	= PPV	= 20 kW/m³
Solar cell blanket power per unit area	= Π	= 300 W/m²
Blanket thickness	= t_b	= 1.3 mm (0.05")
Resultant volume fraction of blanket	= (PPV t_b)/Π	= 0.087 or 8.7%
Solar array blanket area density	= bd	= 1 kg/m²
Resultant blanket power per unit mass	= Π/bd	= 300 W/kg

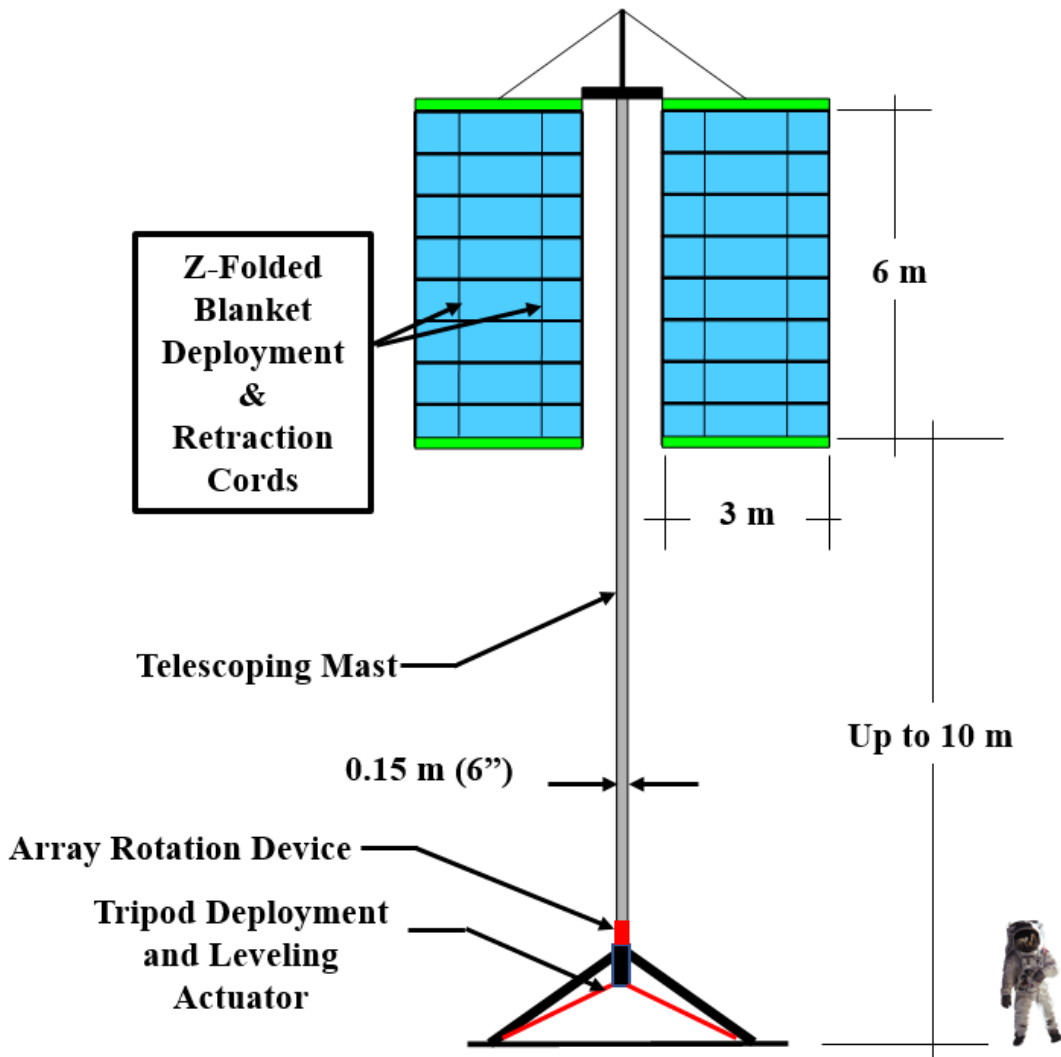


Figure 1. Schematic of a 10 kW Relocatable Solar Array (RSA)

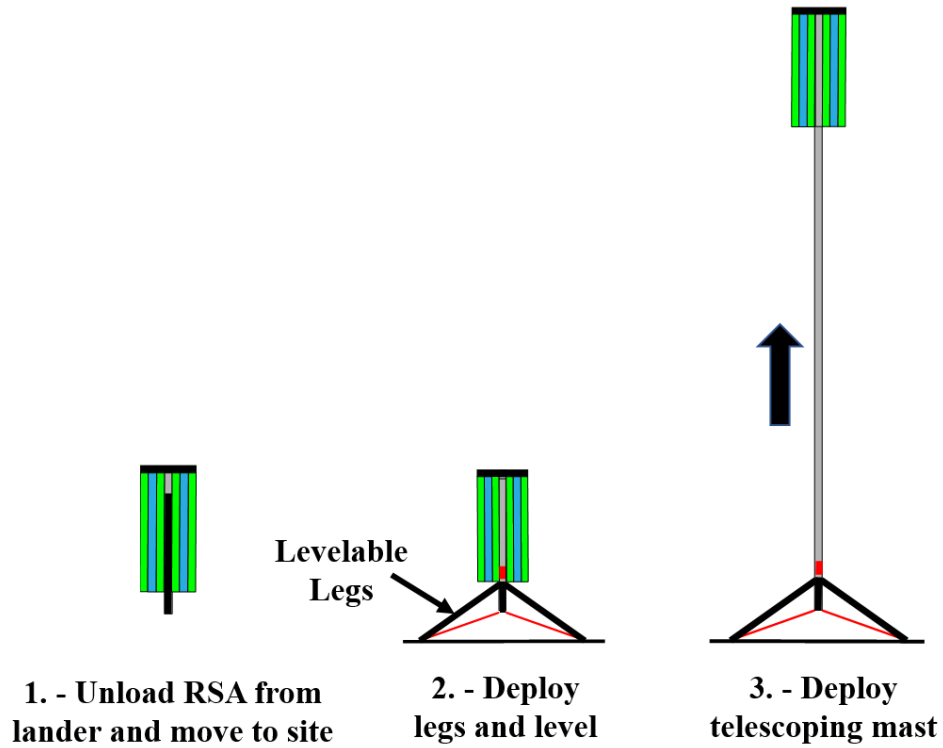


Figure 2. First Three Steps of RSA Deployment Sequence

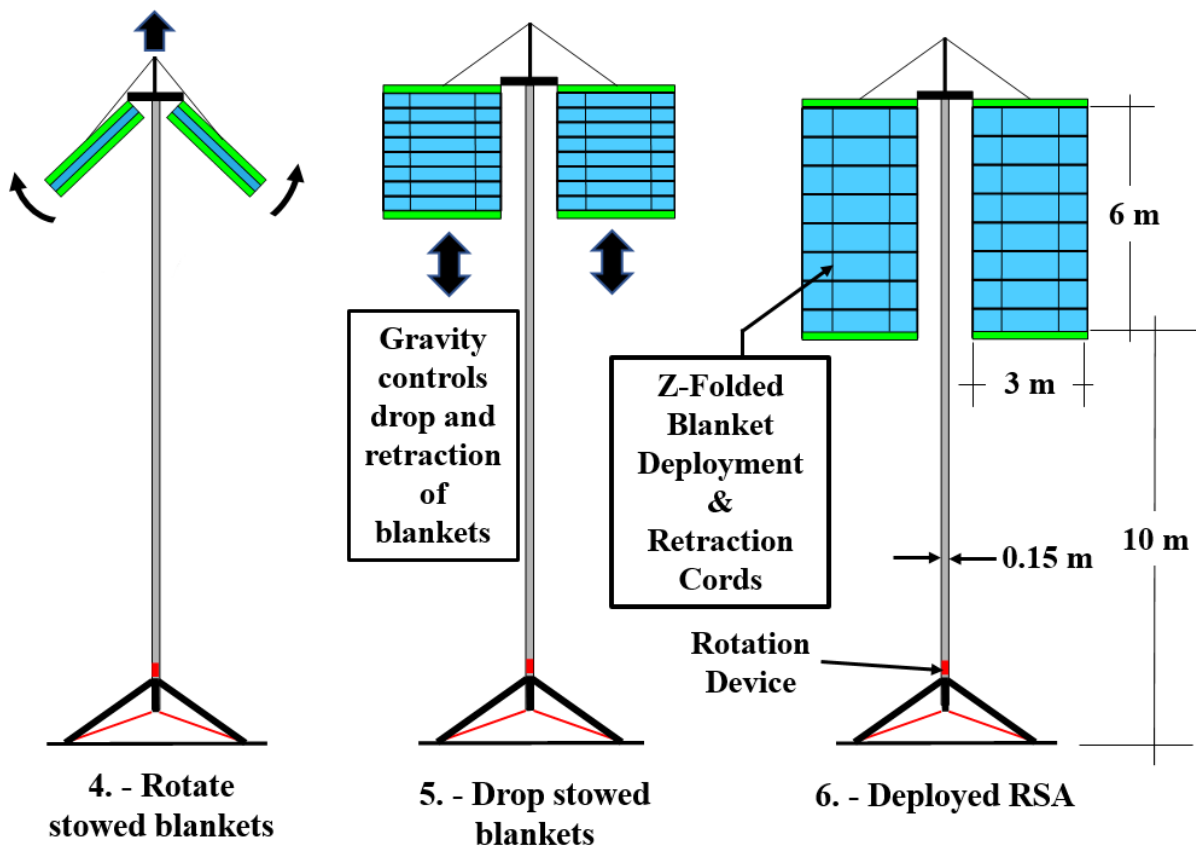


Figure 3. Last Three Steps of RSA Deployment Sequence

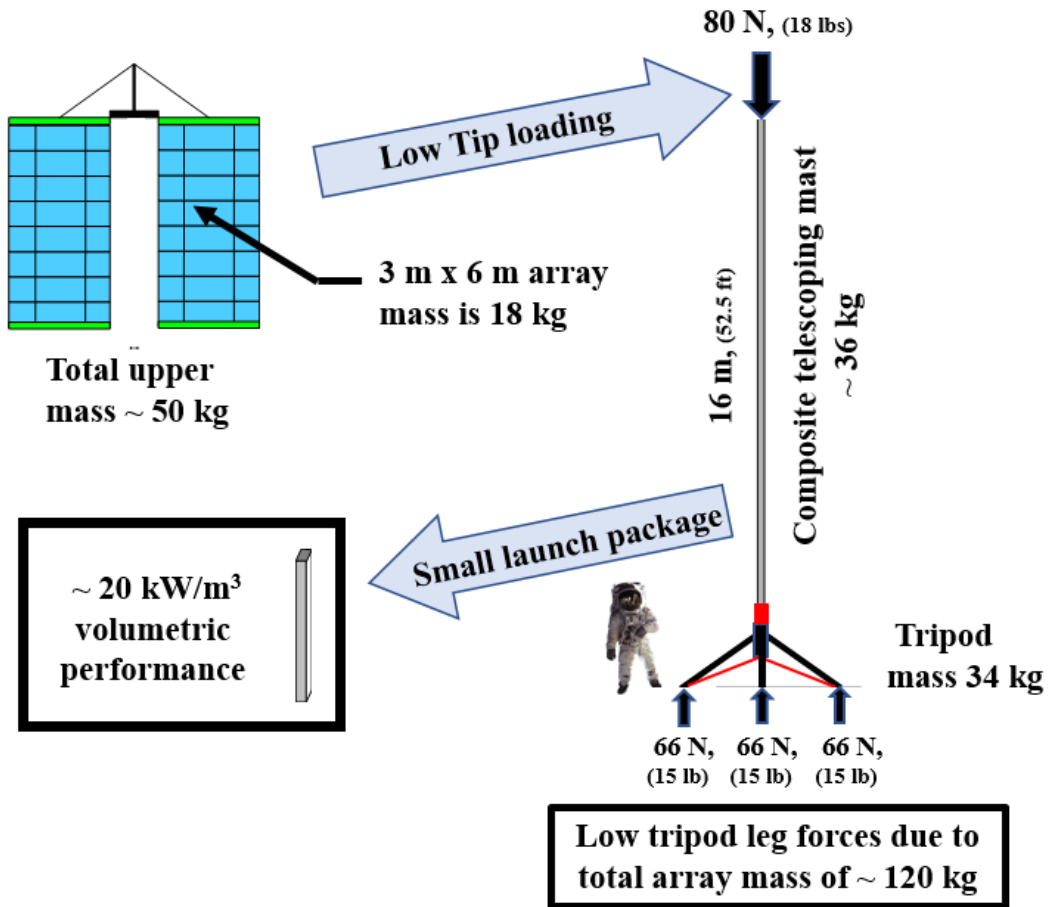


Figure 4. Order-of-Magnitude Summary of Masses, Resulting Loads, and Packing Volume

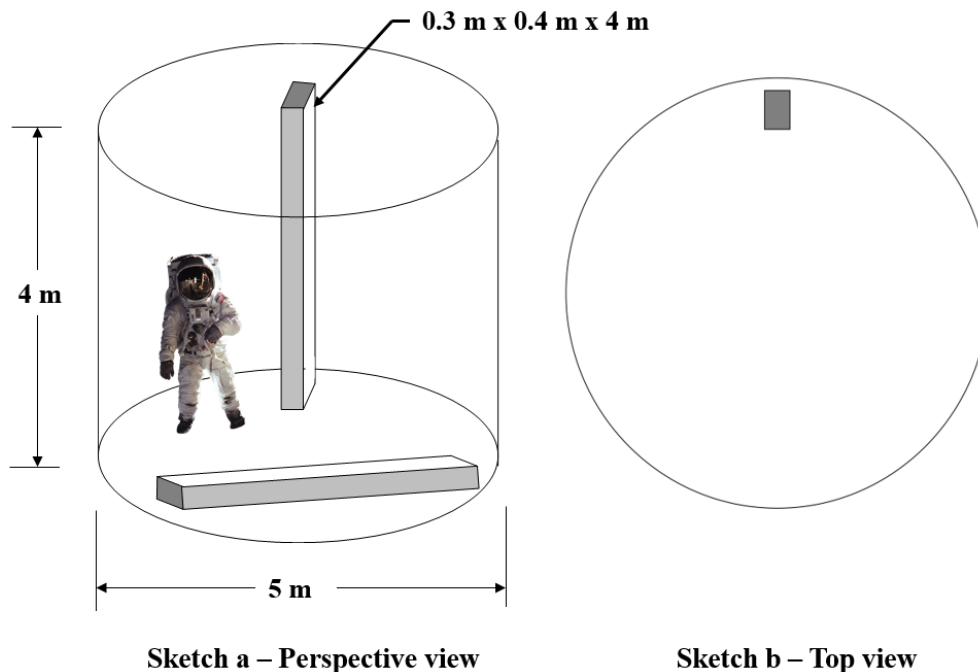


Figure 5. 10 kW Packaged Array at 20 kW/m³ Shown in a 5 m Diameter Launch Shroud

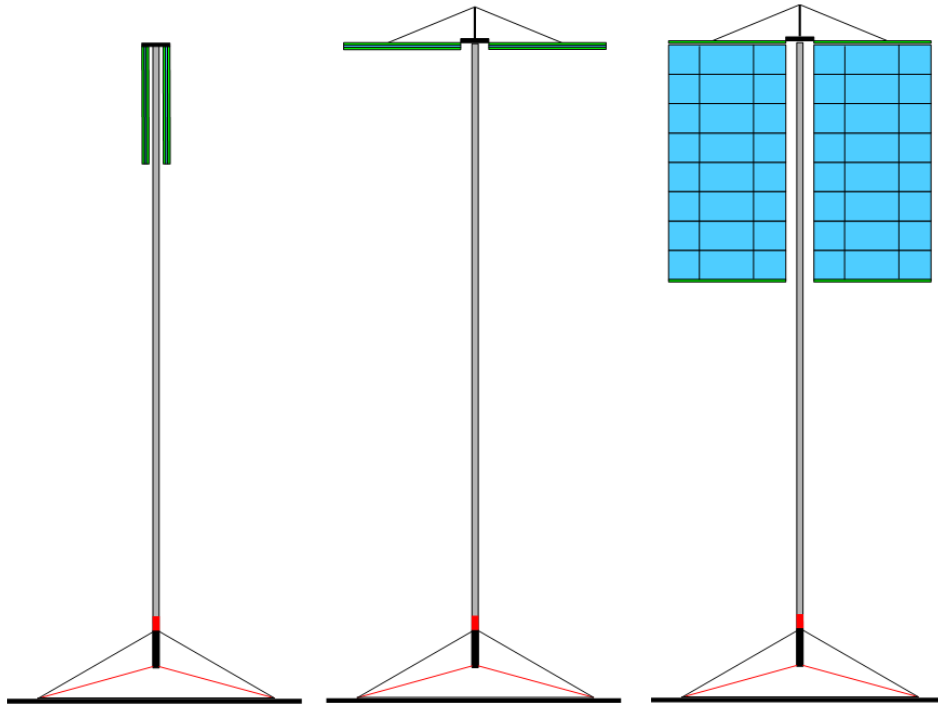


Figure 6. Three Steps of RSA Deployment Showing Slenderness of Structural Members Required to Achieve the Volumetric Packaging Goal of 20 kW/m³

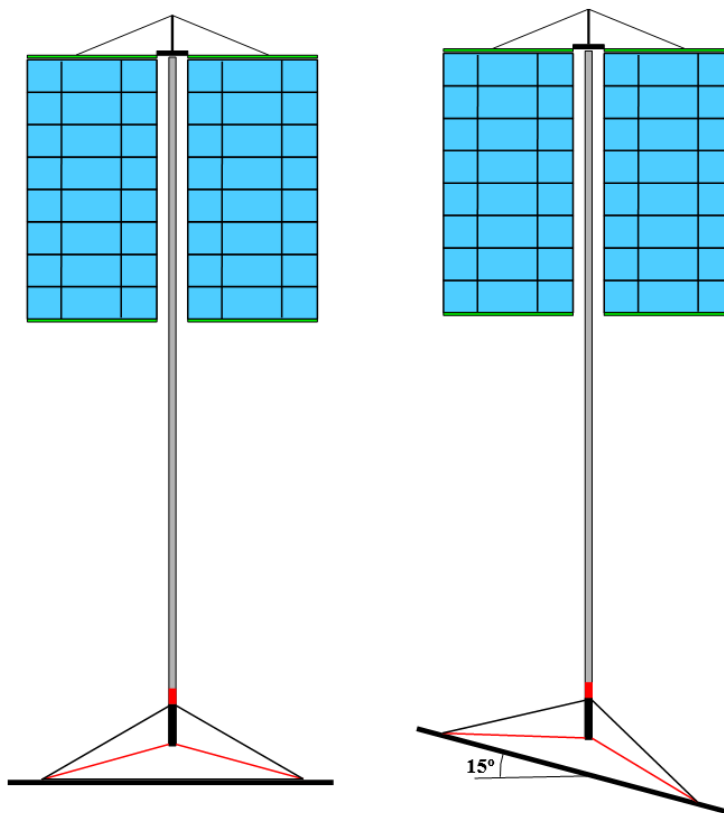


Figure 7. Actuator Length Change When Conforming to Required 15° Surface Slope

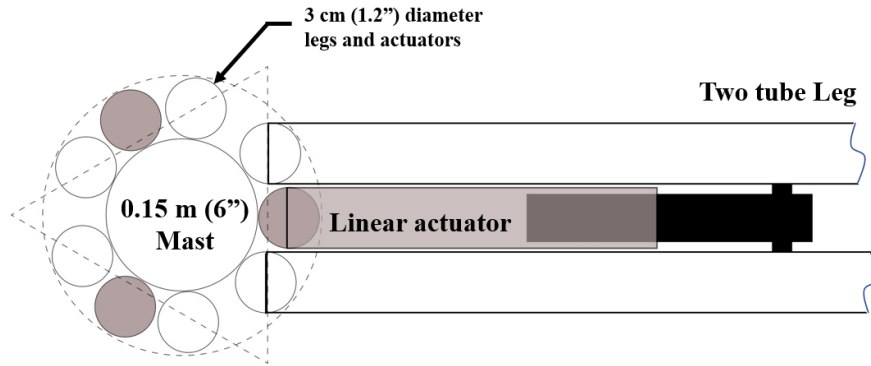


Figure 8. Two-Tube Leg Concept Top View Showing Nested Linear Screw Jack Actuator

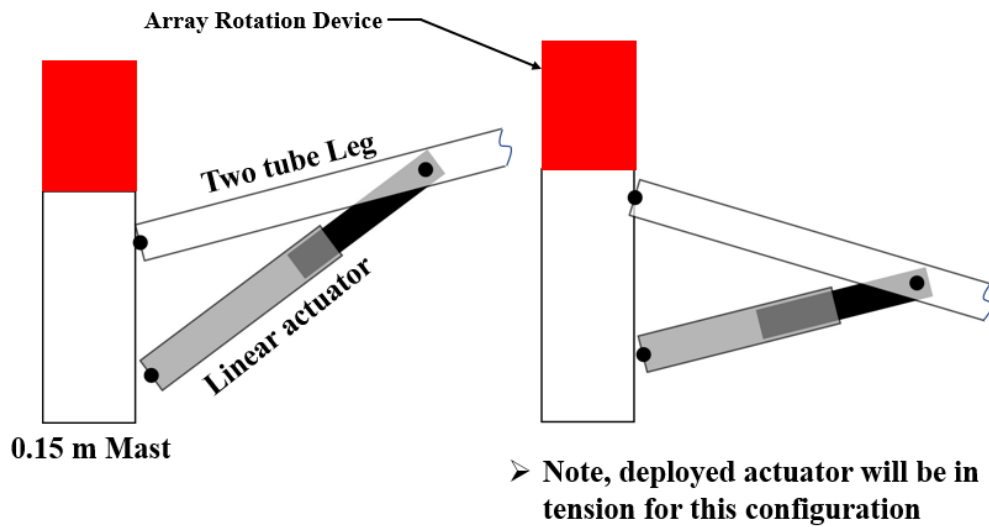


Figure 9. Two-Tube Leg Concept in Two Positions to Illustrate Nested Actuator Operation

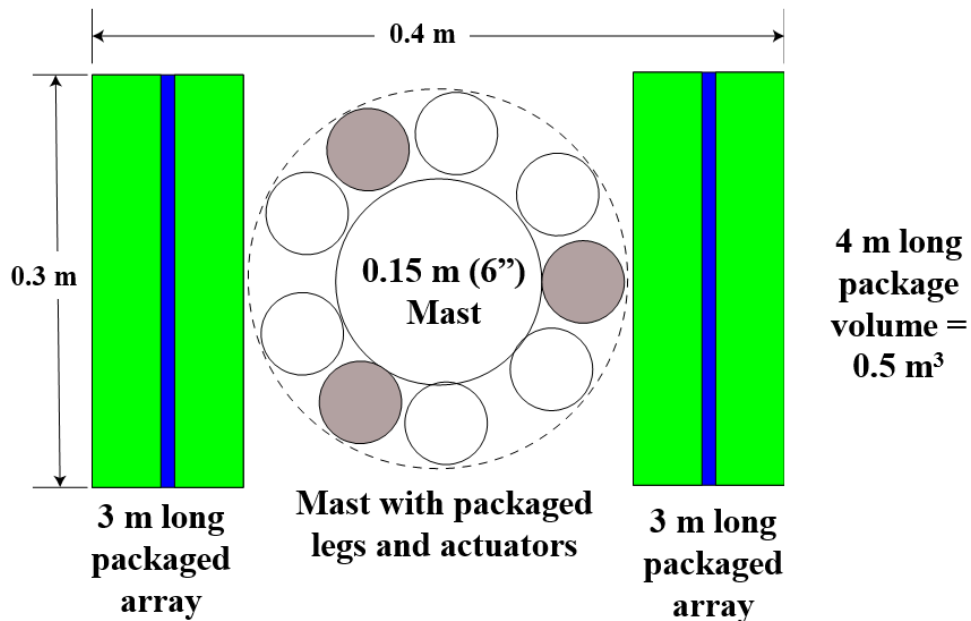


Figure 10. Top View of RSA Launch Package to Achieve 20 kW/m³ Volumetric Efficiency

Table B1. Thermal Properties for Graphite Epoxy Composite

Emissivity	0.84
Absorptivity	0.92
Density	1576 kg/m³
Specific Heat	1044 J/kg-K
Conductivity	1.73 W/m-K

Table B2. Hot-Side and Cold-Side Temperatures for Graphite Epoxy Mast

Diameter	Max Temp (Sun Facing Side)	Min Temp (Shaded Side)
0.20 m	430.8 K (315.8 °F)	207.2 K (-86.7 °F)
0.15 m	425.9 K (306.9 °F)	212.1 K (-77.9 °F)
0.10 m	413.8 K (285.2 °F)	224.2 K (-56.1 °F)

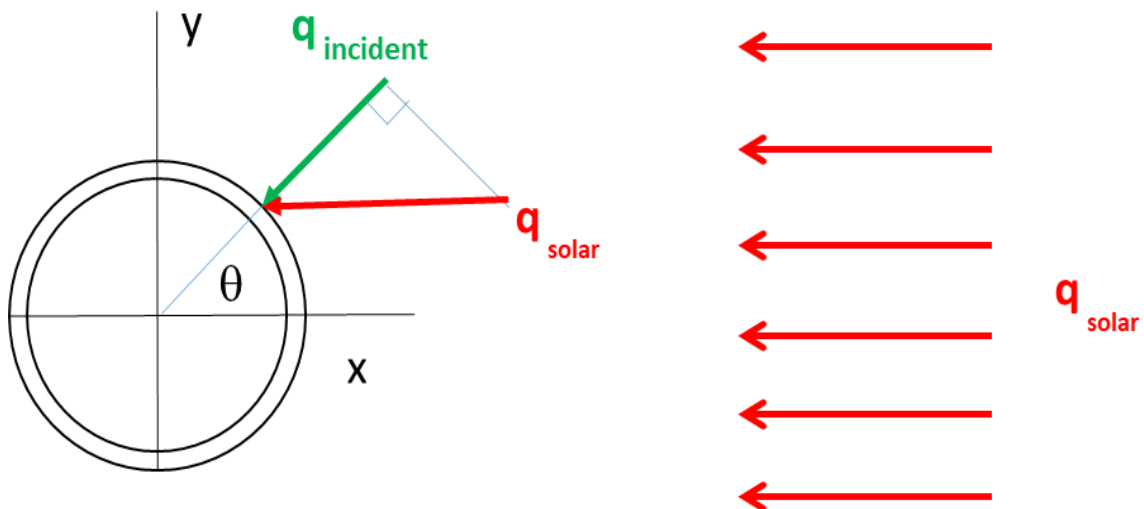


Figure B1. Solar Heating Vector With Respect to the Mast Surface

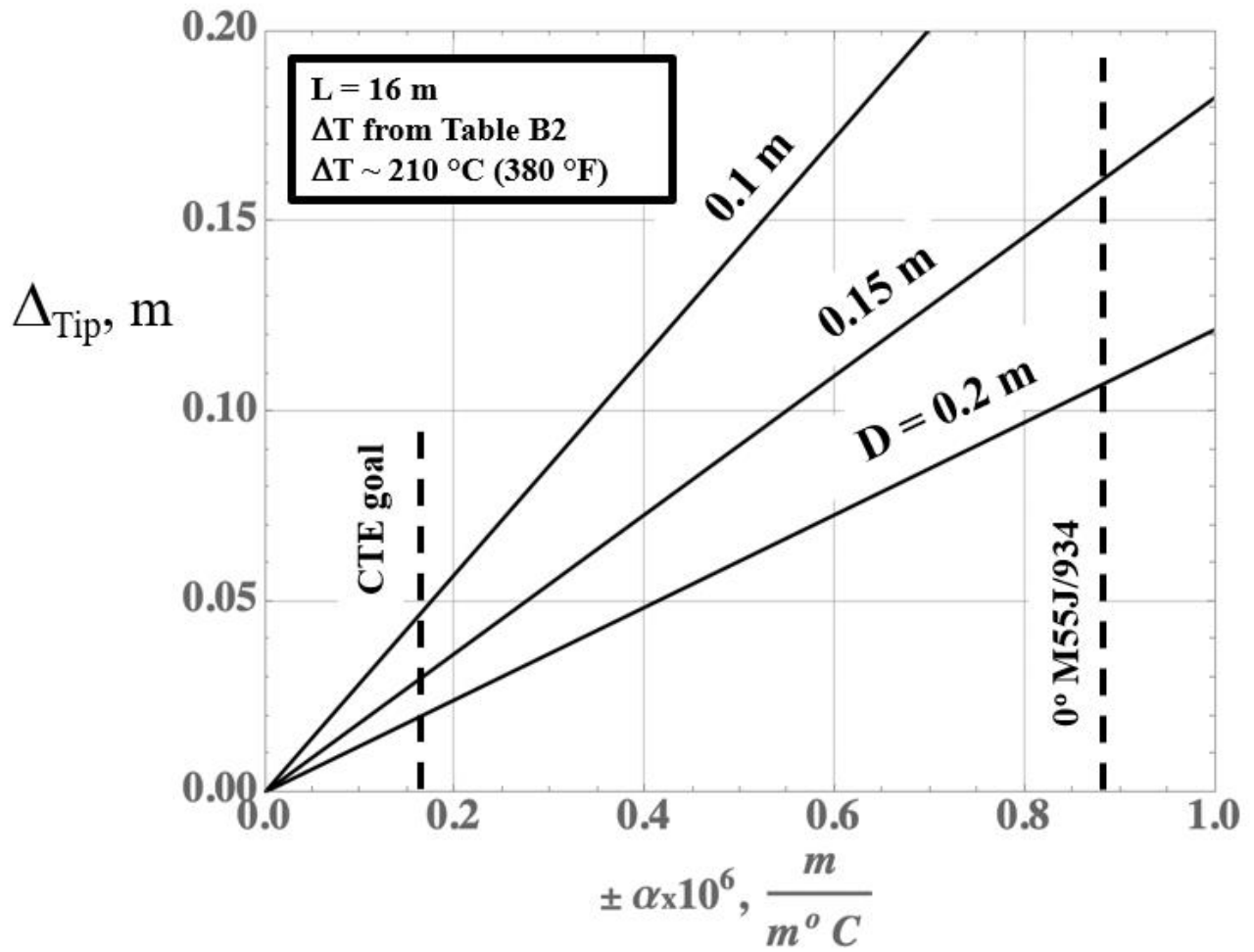


Figure B2. Thermal Tip Deflection vs Coefficient of Thermal Expansion (CTE)

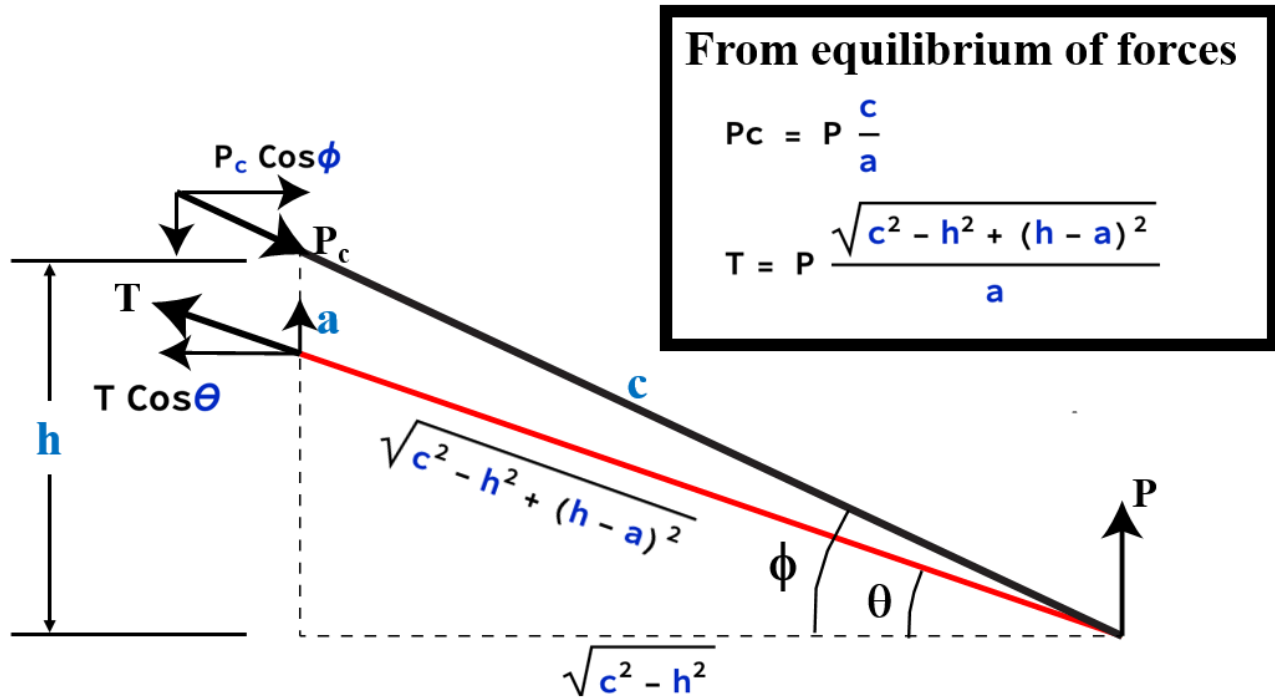


Figure C1. Geometry and Free-Body Diagram of Single Support Tripod Leg and Actuator

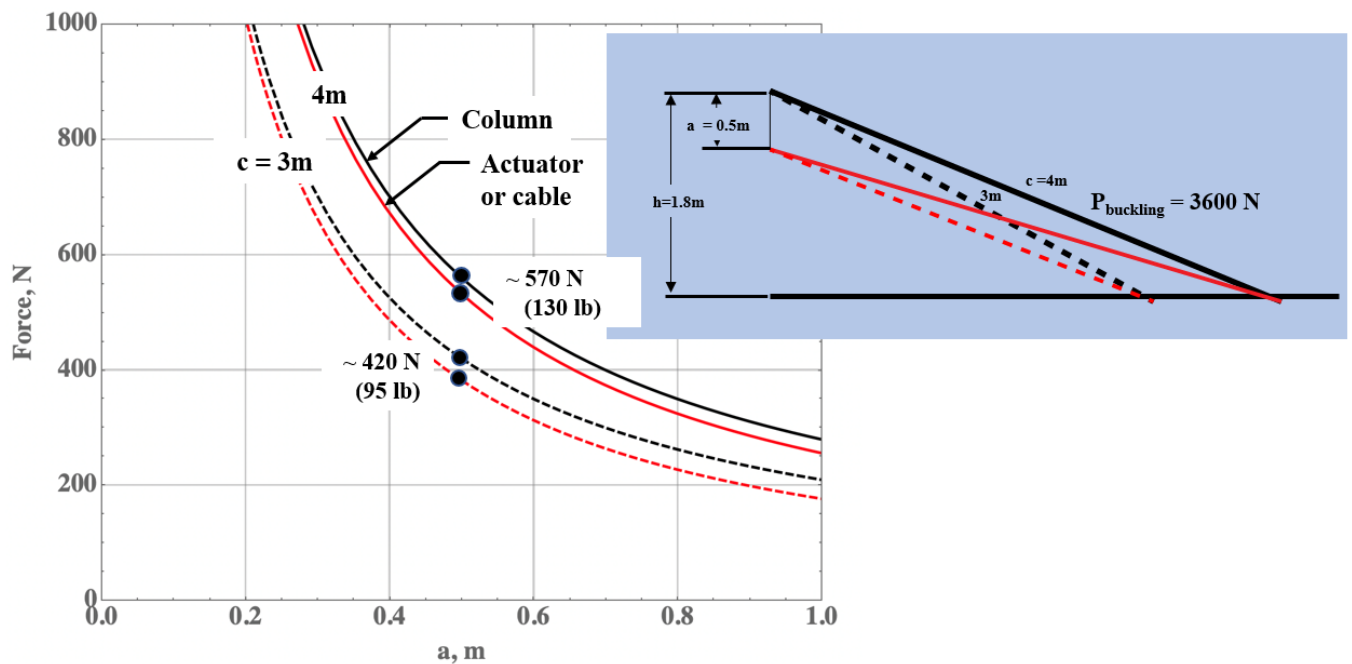


Figure C2. Geometry and Free-Body Diagram of Single Support Tripod Leg and Actuator

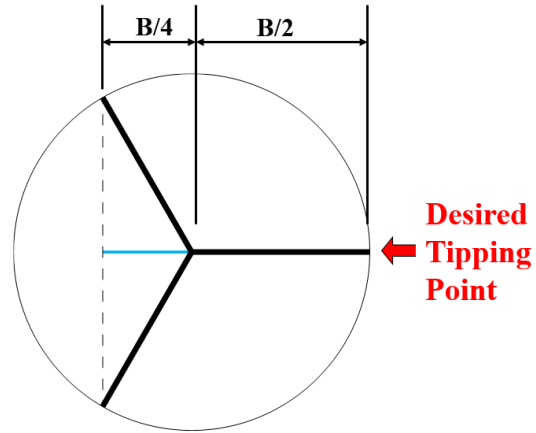


Figure D1. Top View of Desired Metastable Tipping Point for a Tilted RSA

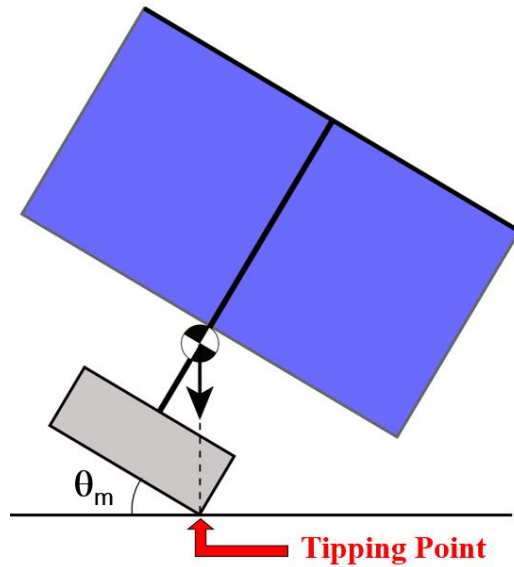


Figure D2. Side View of Desired Metastable Tipping Point for a Tilted RSA

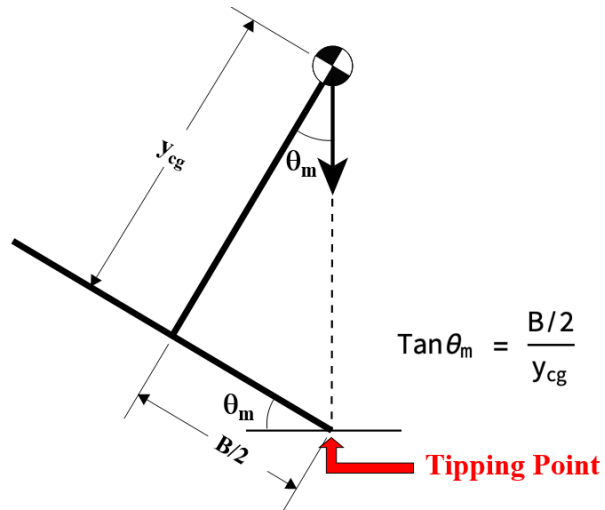
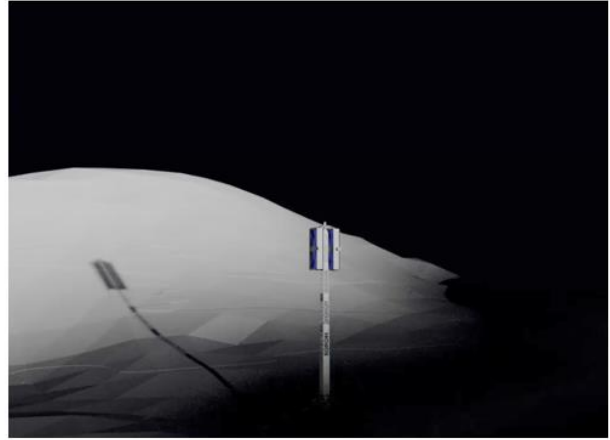


Figure D3. Geometry and Free-Body Diagram of Single Support Tripod Leg and Actuator



1. - Deploy Legs and Level



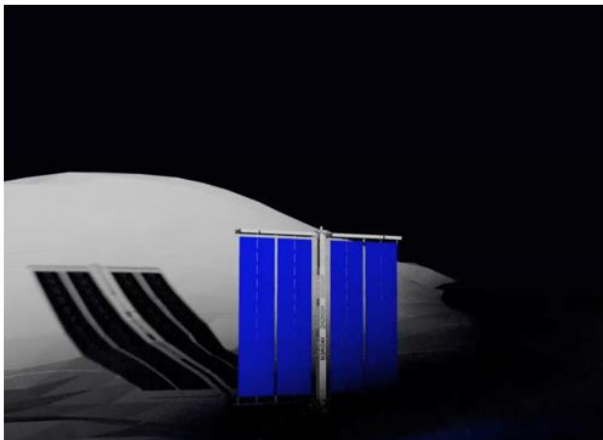
2. - Deploy Telescoping Mast to Minimum Height



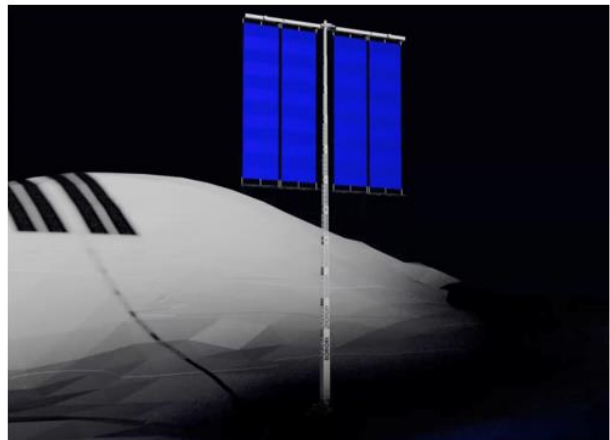
3. - Partially Rotated Blanket Panels



4. - Fully Rotated Blanket Panels



5. - Drop stowed blankets



6. - Deploy Telescoping Mast to Maximum Height

Figure E1. RSA Deployment Sequence with Four Blankets and Variable-Length Central Mast



Figure F1. Photograph of an ISS Solar Array Wing

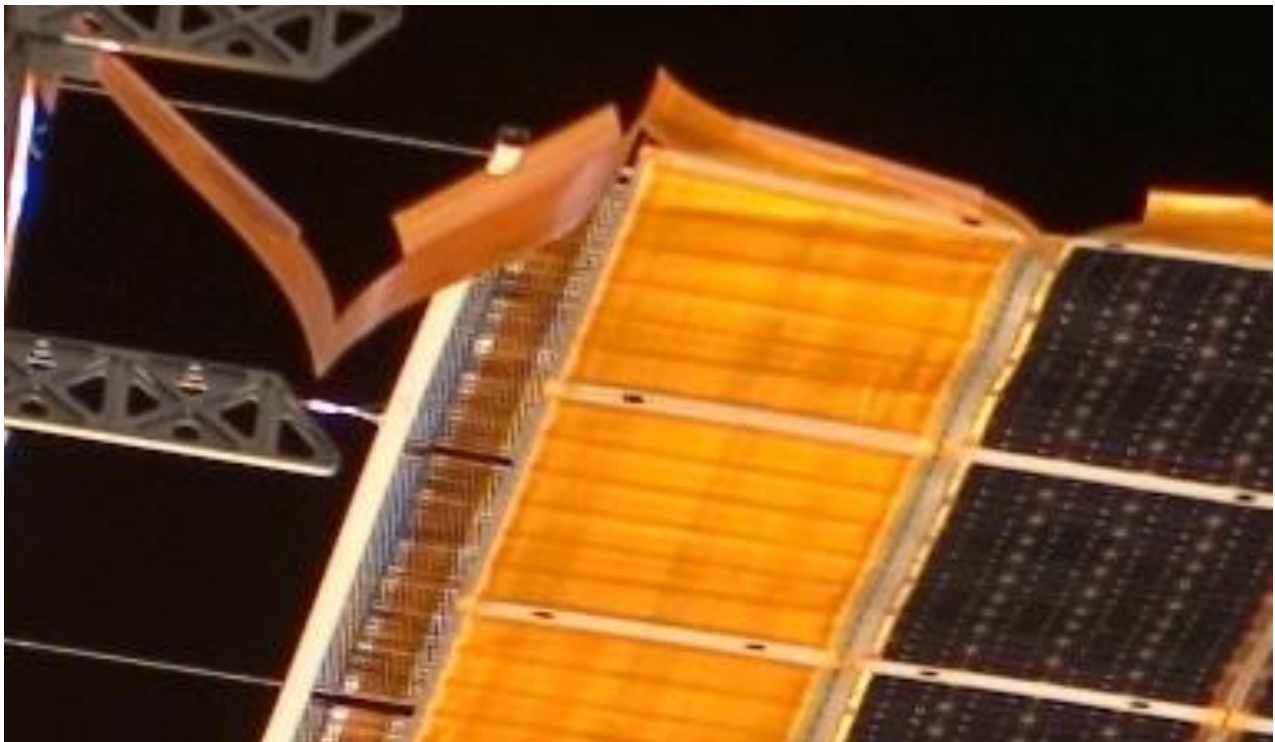


Figure F2. Closeup of an ISS Solar Array Wing Z-Fold Harness

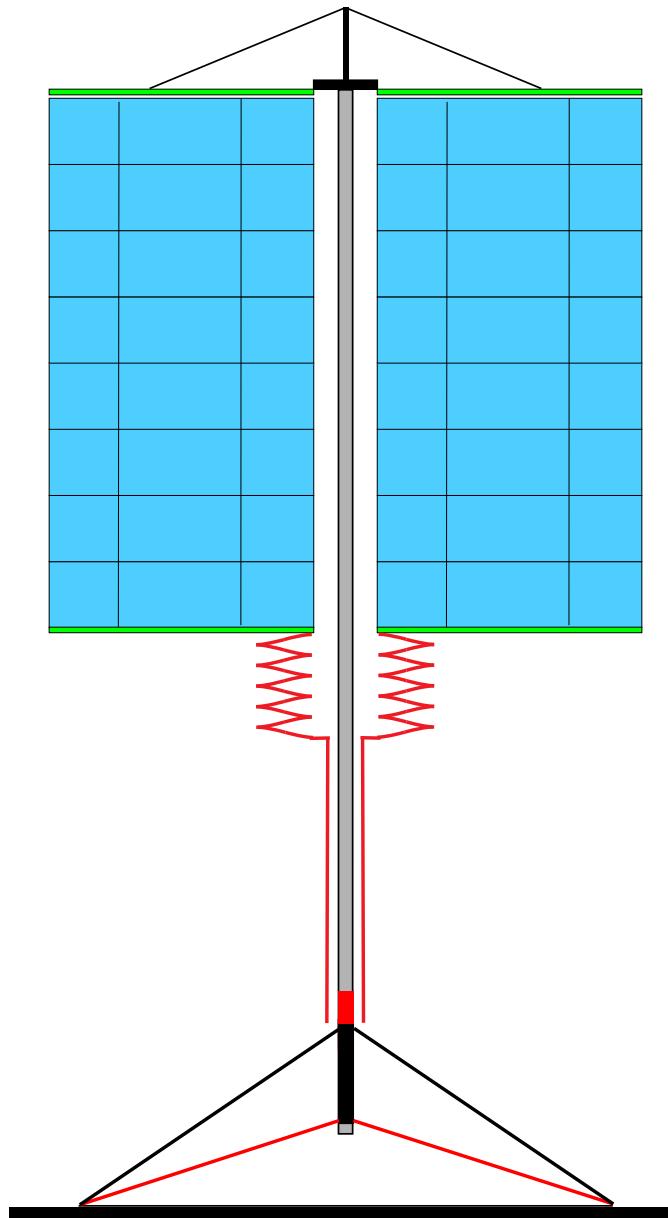


Figure F3. A 10 kW Lunar Solar Array with Partially Deployed Z-Fold Harness

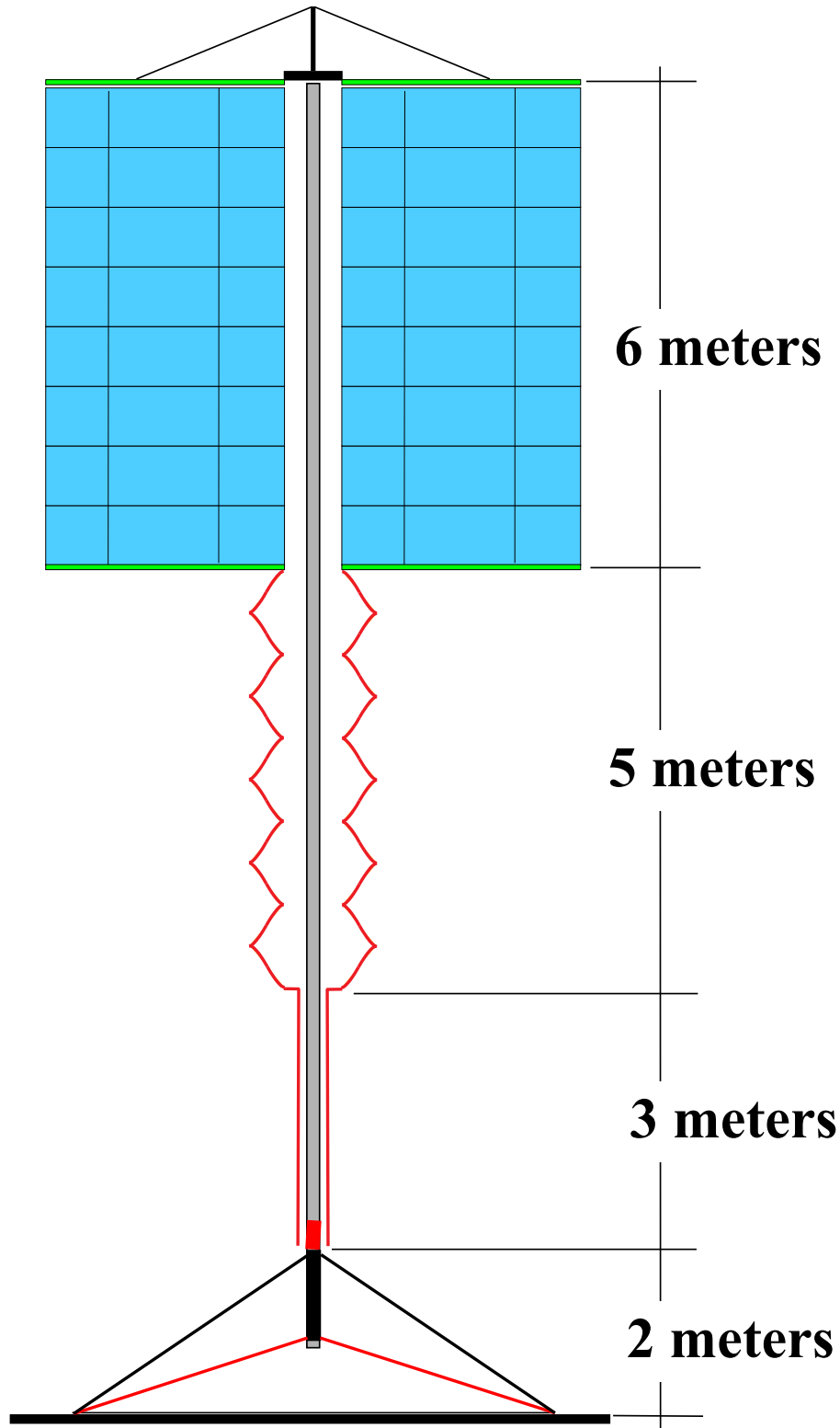


Figure F4. Fully Deployed Lunar 10 kW Solar Array Blankets and Z-Fold Harness

REPORT DOCUMENTATION PAGE

Form Approved
OMB No. 0704-0188

The public reporting burden for this collection of information is estimated to average 1 hour per response, including the time for reviewing instructions, searching existing data sources, gathering and maintaining the data needed, and completing and reviewing this collection of information. Send comments regarding this burden estimate or any other aspect of this collection of information, including suggestions for reducing this burden to Department of Defense, Washington Headquarters Services, Directorate for Information Operations and Reports (0704-0188), 1215 Jefferson Davis Highway, Suite 1204, Arlington, VA 22202-4302. Respondents should be aware that notwithstanding any other provision of law, no person shall be subject to any penalty for failing to comply with a collection of information if it does not display a currently valid OMB control number. **PLEASE DO NOT RETURN YOUR FORM TO THE ABOVE ADDRESS.**

1. REPORT DATE (DD-MM-YYYY) 3-29-2021		2. REPORT TYPE Technical Memorandum		3. DATES COVERED (From - To)	
4. TITLE AND SUBTITLE Relocatable 10 kW Solar Array for Lunar South Pole Missions				5a. CONTRACT NUMBER	
				5b. GRANT NUMBER	
				5c. PROGRAM ELEMENT NUMBER	
6. AUTHOR(S) Richard Pappa, Chuck Taylor, Jay Warren, Matt Chamberlain, Sarah Cook, Scott Belbin, Roger Lepsch, Dan Tiffin, Bill Doggett NASA Langley Research Center, Hampton, VA Martin Mikulas, Iok Wong - National Institute of Aerospace, Hampton, VA Dave Long, Devon Steinkoenig, Alejandro Pensado - Analytical Mechanics Associates, Hampton, VA Joseph Blandino, Jerry Haste - Virginia Military Institute, Lexington, VA				5d. PROJECT NUMBER	
				5e. TASK NUMBER	
				5f. WORK UNIT NUMBER WBS 596118.04.61.23	
7. PERFORMING ORGANIZATION NAME(S) AND ADDRESS(ES) AND ADDRESS(ES) NASA Langley Research Center Hampton, VA 23681-2199				8. PERFORMING ORGANIZATION REPORT NUMBER	
9. SPONSORING / MONITORING AGENCY NAME(S) AND ADDRESS(ES) National Aeronautics and Space Administration Washington, DC 20546-001				10. SPONSOR/MONITOR'S ACRONYM(S) NASA	
				11. SPONSOR/MONITOR'S REPORT NUMBER(S) NASA/TM-20210011743	
12. DISTRIBUTION / AVAILABILITY STATEMENT Unclassified - Unlimited Subject Category Availability: NASA STI Program (757) 864-9658					
13. SUPPLEMENTARY NOTES					
14. ABSTRACT Deployable, relocatable, free-standing solar arrays are being developed to provide modular power for future lunar South Pole missions. Major design requirements for these arrays will be low mass, compact launch stowage, and highly reliable deployment and retraction. This paper presents a novel conceptual design for a 10 kW solar array to address these requirements referred to as the Relocatable Solar Array (RSA). Simply stated, the concept is a pair of solar cell blankets freely hanging from a horizontal cross arm supported by a vertical, slender, telescoping mast resting on a deployable tripod base. A major factor in simplifying the design is that the force exerted by lunar gravity is used to deploy and maintain extension of the hanging array blankets. A second major factor in achieving the desired low mass and high volumetric efficiency is that the array operates in the vacuum, low-gravity, lunar environment with no deployed vibration frequency requirement. Such a low-load environment enables use of extraordinarily slender and low mass structural members to support the hanging array blankets. This concept was developed, in part, to serve as a NASA reference solar array concept against which other proposed arrays can be compared.					
15. SUBJECT TERMS Lunar Surface Power, Deployable Solar Arrays, Relocatable Solar Arrays, High Power Flexible-Substrate Solar Arrays					
16. SECURITY CLASSIFICATION OF:			17. LIMITATION OF ABSTRACT UU	18. NUMBER OF PAGES 31	19a. NAME OF RESPONSIBLE PERSON HQ - STI-infodesk@mail.nasa.gov
a. REPORT U	b. ABSTRACT U	c. THIS PAGE U			19b. TELEPHONE NUMBER (include area code) 757-864-9658